Supplementary Information: Suppressing the Rebound of Impacting Droplets from Solvophobic Surfaces by Polymer Additives: Polymer Adsorption and Molecular Mechanisms

Eunsang Lee[1], Hari Krishna Chilukoti[1,2], and Florian Müller-Plathe[1]

[1]Eduard-Zintl-Institut für Anorganische und Physikalische Chemie, Technische Universität Darmstadt, Alarich-Weiss-Strasse 8, 64287, Darmstadt, germany
[2]Current affiliation: Department of Mechanical Engineering, National Institute of Technology Warangal, Warangal, Telangana 506004, India

S1 Solvent Quality of Polymer Solution

Table S1: Simulation parameters for different bead types. Subscripts S, P, and W indicate solvent, polymer and substrate beads, respectively.

	A	r_{A}	B	r_{B}
S/S	-40	1.00	25	0.75
P/P	-40	1.00	25	0.75
S/P	-40	1.00	25	0.75
S/W	-10	1.00	25	0.75

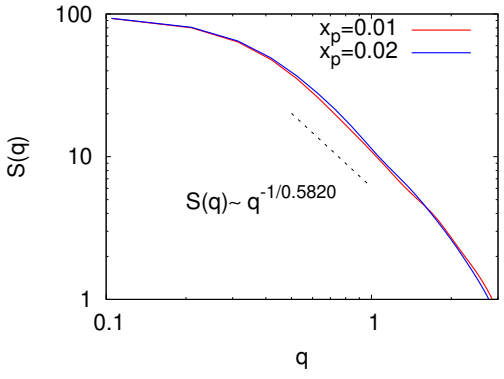

Figure S1: Single molecule structure factor of $N_{\mathrm{p}} = 100$, $x_{\mathrm{p}} = 0.010$ and 0.020. A dashed line indicate the fitted function by $S(q) \sim -q^{1/\nu}$. A dashed line shows the scaling of $S(q) \sim q^{-1/\nu}$, where ν is a Flory exponent in a good solvent condition. Reprinted with permission from [Lee et al, *ACS Macro Lett.* **2021**, 10, 192-196][1]. Copyright @ American chemical Society.

Our simulation model is composed of solvent (subscripted by S), polymer (P) and substrate (W) beads. Repulsion parameters, B and r_{B}, are same regardless of types of pair (Tab. S1). Attraction parameters are chosen to mimic athermal solvent conditions indicating a negative Flory-Huggins parameter at any non-zero temperature. This is achieved by setting the interaction parameters between solvent/solvent, solvent/polymer and polymer/polymer identical. We confirm that our choice of parameters reproduces well the Flory exponent $\nu \approx 0.588$ for a good solvent condition (Figure S1).

S2 Equilibrium Properties of Free Droplet

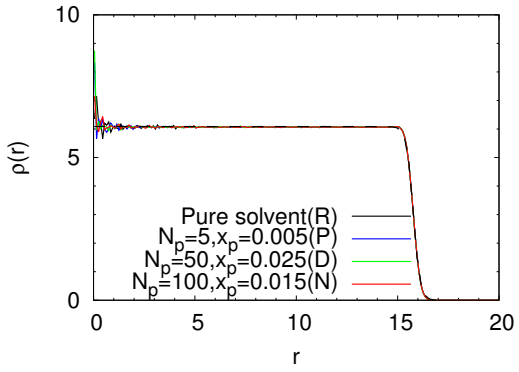

Figure S2: Particle number density as a function of distance from the center of droplet for different droplets. All curves merge in a single curve. A dashed line represents the fitted function of Eqn. 1.

We calculate equilibrium properties of free droplets to calculate Reynolds (Re= $D_0 v_{\mathrm{imp}} \rho / \eta_{\mathrm{s}}$) and Weber numbers (We= $D_0 v_{\mathrm{imp}}^2 \rho / \sigma$), where D_0 is the equilibrium droplet diameter, ρ is the droplet mass density, η_{s} is the shear viscosity, and σ is the fluid's liquid-vapor surface tension.

Figure S2 shows the radial number density of liquid beads (ρ_{r}) as a function of distance from the droplet center for different polymer compositions. We fit ρ_{r} with the following function:

$$\rho_{\mathrm{r}}(r) = \frac{\rho_{\mathrm{l}} + \rho_{\mathrm{v}}}{2} - \frac{\rho_{\mathrm{l}} + \rho_{\mathrm{v}}}{2} \tanh \frac{2(r - D_0/2)}{\delta}, \tag{1}$$

where ρ_{l}, ρ_{v}, D_0, δ are the liquid density, the vapor density, the equilibrium droplet diameter, and the interface width, respectively. The resulting droplet density $\rho = \rho_{\mathrm{l}} = 6.09$ and the equilibrium diameter $D_0 = 31.6$ are constant regardless of polymer composition.

We also calculate the zero-shear viscosity from separate bulk solution simulations. After preparing systems of 10^6 liquid particles containing the same polymer composition and the same particle density as the droplet, we perform equilibrium simulations for $10^4\tau$. The zero-shear viscosity η_0 is calculated by integrating the stress auto-correlation function given by

$$\eta_0 = \frac{V}{k_{\mathrm{B}}T} \int_0^\infty G(t)\mathrm{d}t = \frac{V}{k_{\mathrm{B}}T} \int_0^\infty \langle \sigma_{\mu\nu}(t) \cdot \sigma_{\mu\nu}(0) \rangle \mathrm{d}t, \tag{2}$$

$\sigma_{\mu\nu}$ being off-diagonal element of the stress tensor, $\mu \neq \nu$. Figure 3(a) shows the stress auto-correlation function $G(t)$ for different polymer solutions. Even for the longest polymer, N_{p}=100 at the highest concentration, $x_{\mathrm{p}} = 0.025$, the stress mostly decays in a very short time, faster than 1τ. Considering the relaxation time of the polymer for N_{p}=100 of about 1600τ (Figure 3(b)), the

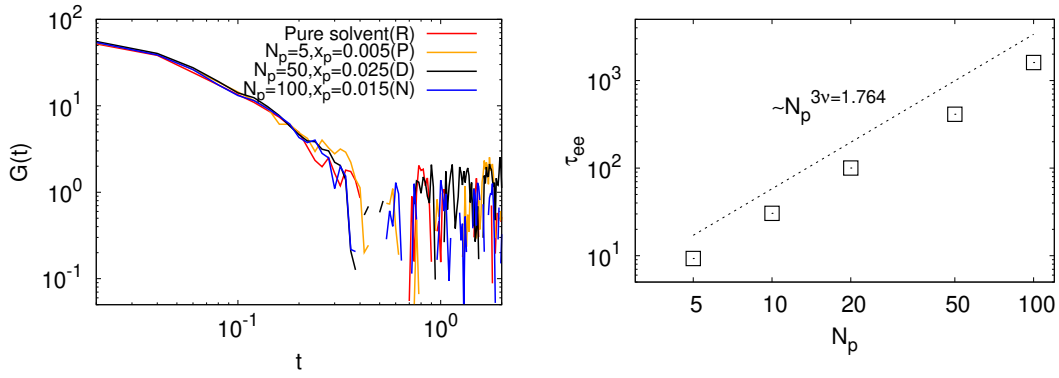

(a) (b)

Figure S3: (a) Stress auto-correlation function for different polymer solutions and (b) the end-to-end relaxation time of polymer as a function of N_p at $x_\mathrm{p} = 0.025$. τ_ee at different concentration is not different from the result shown here. In (b), a dashed line shows the scaling of $\tau_\mathrm{ee}(N_\mathrm{p}) \sim N_\mathrm{p}^{3\nu}$, where ν is a Flory exponent in a good solvent condition. Reprinted with permission from [Lee et al, *ACS Macro Lett.* **2021**, 10, 192-196][1]. Copyright @ American chemical Society.

Table S2: Calculated zero-shear viscosity for different polymer lengths and concentrations. Errors are given in the parenthesis.

N_p \ x_p	0.005	0.010	0.015	0.020	0.025
Pure solv.			6.68 (± 0.85)		
5	6.91 (± 0.94)	6.90 (± 0.80)	6.28 (± 0.68)	6.42 (± 0.66)	6.22 (± 0.87)
10	7.62 (± 0.71)	6.85 (± 0.90)	6.68 (± 0.59)	7.21 (± 0.45)	6.76 (± 0.70)
20	7.23 (± 0.69)	6.79 (± 0.85)	7.01 (± 0.90)	6.44 (± 0.69)	7.15 (± 0.73)
50	6.89 (± 0.88)	7.40 (± 0.78)	7.80 (± 1.03)	7.17 (± 0.60)	6.96 (± 0.92)
100	7.07 (± 0.79)	6.76 (± 0.95)	6.41 (± 0.80)	6.28 (± 0.81)	7.66 (± 0.93)

polymer contribution to the solution viscosity is negligible. The resulting η_0's are listed in Tab. S2, but there is no clear trend of it depending on N_p and x_p due to very small η_0. Thus, the polymer contribution to the solution viscosity is very small and almost identical for all systems under investigation.

We calculate liquid-vapor surface tension of a droplet using the radial distance-dependent pressure tensor calculated by the Irving-Kirkwood method:[2]

$$p_{\mu\nu}(r) = \langle\rho(r)\rangle k_\mathrm{B}T\ \mathbf{I} + \frac{1}{A}\Big\langle \sum_{i>j} (\mathbf{r}_{ij})_\mu (\mathbf{f}_{ij})_\nu \theta\big(\frac{r - r_i}{r_{ij}}\big)\theta\big(\frac{r_j - r}{r_{ij}}\big)\Big\rangle, \tag{3}$$

where $\mathbf{I}$ is the unit tensor, $\mathbf{r}_{ij}$ and $\mathbf{f}_{ij}$ is the relative distance and force vectors between particles i and j, respectively. $\theta(x)$ is the Heaviside functions. For a spherical interface, the surface tension is calculated from the pressure tensor in the spherical coordinate where the origin is the center of a droplet. Therefore, we transform $\mathbf{r}$ and $\mathbf{f}$ into spherical polar coordinates and obtain radial (p_{rr}) and tangential components of the pressure tensor ($p_{\theta\theta}$ and $p_{\phi\phi}$) as a function of distance from the

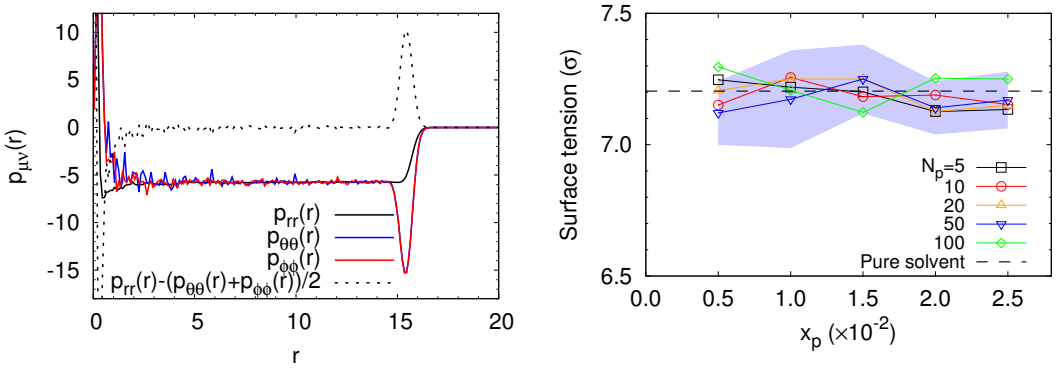

Figure S4: (a) Radial and tangential components of the pressure tensor as a function of distance from the center of a droplet. This figure is obtained from the droplet of $N_\mathrm{p} = 5$ and $x_\mathrm{p} = 0.025$. (b) Surface tension as a function of x_p for different N_p. Error colored by shaded area is shown only for $N_\mathrm{p} = 50$ droplets. The black dashed line indicates the surface tension of a pure solvent droplet.

Table S3: Reynolds and Weber numbers of free droplets. Errors are given in the parenthesis.

N_p \ x_p	0.005	0.010	0.015	0.020	0.025
			Re		
Pure solv.			57.4 (± 7.3)		
1			57.5 (± 7.3)		
5	55.6 (± 7.6)	56.7 (± 6.6)	61.2 (± 6.6)	59.9 (± 6.2)	61.8 (± 8.6)
10	57.4 (± 5.3)	56.2 (± 7.4)	57.5 (± 5.0)	53.2 (± 3.3)	56.8 (± 5.8)
20	53.1 (± 5.1)	56.4 (± 7.1)	54.1 (± 6.9)	59.5 (± 6.4)	53.7 (± 5.5)
50	55.6 (± 7.1)	51.9 (± 5.5)	49.5 (± 7.3)	53.4 (± 4.5)	55.2 (± 7.3)
100	54.3 (± 6.1)	56.7 (± 8.0)	60.0 (± 7.5)	61.1 (± 7.8)	50.2 (± 6.1)
			We		
Pure solv.			106.4 (± 2.0)		
1			107.5 (± 2.0)		
5	106.2 (± 2.3)	106.4 (± 2.8)	106.7 (± 2.0)	107.9 (± 2.2)	107.8 (± 1.8)
10	107.5 (± 2.1)	106.0 (± 2.3)	107.0 (± 3.1)	106.6 (± 2.9)	107.3 (± 3.1)
20	106.4 (± 3.1)	105.6 (± 3.0)	105.8 (± 3.4)	107.5 (± 2.5)	107.5 (± 1.8)
50	107.7 (± 2.6)	107.2 (± 3.9)	106.5 (± 2.7)	107.4 (± 2.1)	107.2 (± 2.3)
100	105.2 (± 3.9)	106.5 (± 2.5)	107.9 (± 2.5)	105.8 (± 3.8)	106.0 (± 2.1)

droplet center. The surface tension is then calculated by:[3]

$$\sigma = \frac{4}{D_0^2}\int_0^\infty \mathrm{d}r^2[p_{rr}(r) - \frac{1}{2}\{p_{\theta\theta}(r) + p_{\phi\phi}(r)\}] \tag{4}$$

Figure 4(a) shows the pressure tensor components as a function of distance from the center of the droplet. The pressure difference near the interface, and the width in which p_{rr} and $p_{\theta\theta}$ (or $p_{\phi\phi}$) differ from each other is the same as the interfacial width in Figure S2. By integrating the difference of the radial and tangential pressures (a dashed line in Figure 4(a), we obtain the surface

tension for different droplets as shown in Fig. 4(b). As expected, the surface tension of different droplets seems to be almost the same within the statistical error, which means that Reynolds and Weber numbers of our droplets are the same without statistically meaningful difference.(Tab. S3)

S3 Molecular Kinetic Theory of Wetting

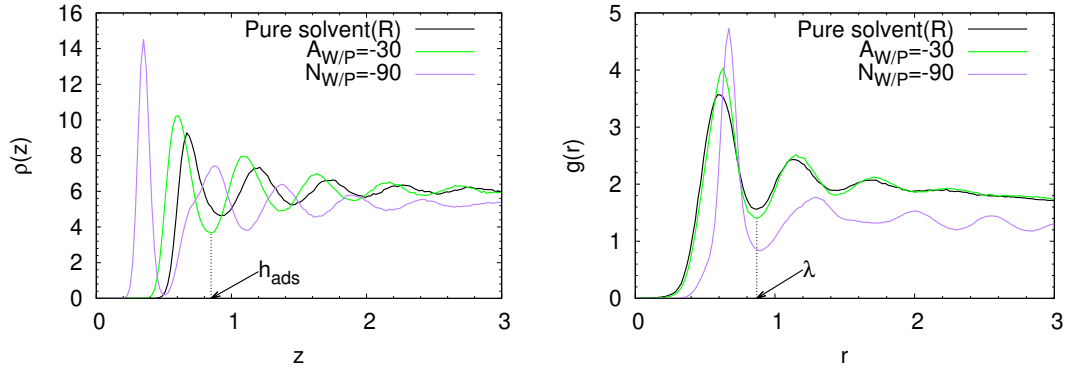

(a) (b)

Figure S5: (a) Particle density profile as a function of a distance from the surface. The first minimum after the first peak indicates the the thickness of the first adsorption layer. (b) Two-dimensional radial distribution function of particles in the first adsorption layer. The first minimum indicates the distance to the nearest neighbor.

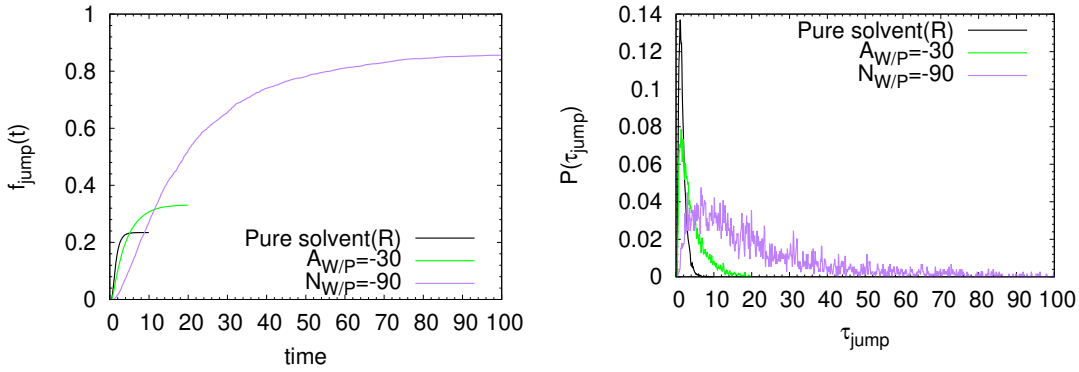

(a) (b)

Figure S6: (a) Cumulative fraction of the particle which moves a distance larger than λ within the first adsorption layer as a function of time. (b) Probability distribution of the molecular jump times.

If a solid-liquid interface were static and homogeneous, that is not the case for our droplets of polymer solution, parameters in Equation 1 in the main article can be evaluated explicitly from the static droplets deposited on the substrate(Table S4).[4] To compare the friction coefficient of the impacting droplet with that from the MKT, we first obtain the thickness of the first adsorption layer, h_{ads}, at which the particle density profile along z-direction has a minimum after the first

Table S4: Parameters for the molecular kinetic theory of wetting. h_{ads} and $\langle\tau_{\mathrm{jump}}\rangle$ mean the thickness of the first adsorption layer and the average time for the molecular jump to the nearest site, respectively.

System	h_{ads}	λ	$\langle\tau_{\mathrm{jump}}\rangle$	κ_0	n	γ	ζ_{CL}	$\zeta_{\mathrm{CL}}/\gamma$
Pure Solvent	0.93	0.87	1.68	0.59	2.32	7.20	4.48	0.62
$A_{\mathrm{P/W}} = -30$	0.85	0.87	4.20	0.24	2.61	7.14	12.61	1.77
$A_{\mathrm{P/W}} = -90$	0.51	0.89	21.22	0.04	0.69	7.14	16.50	2.31

peak (Figure 5(a)). It is obvious that the thickness is smaller for the stronger polymer-surface attraction strength. We also calculate the two-dimensional radial distribution function in the first adsorption layer, and then define the distance of the first minimum correlation as the distance to the nearest adsorption site, λ (Figure 5(b)). Calculated λ's turn out to be almost identical for all systems. To obtain the frequency of a molecular jump, κ_0, we calculate a cumulative fraction of particles which move further than λ within the first adsorption layer as a function of time duration t as in Figure 6(a)($f_{\mathrm{jump}}(t)$). By taking a time derivative of the cumulated fraction, we obtain the (unnormalized) distribution of molecular jump times, $P(t) = \mathrm{d}f_{\mathrm{jump}}(t)/\mathrm{d}t$ (Figure 6(b)). We find a very long tail of the distribution for the system of strong polymer-surface attraction, that is obviously from the contribution of adsorbed polymer beads. Averaging τ_{jump} for $P(\tau_{\mathrm{jump}})$ gives the average time of parallel molecular jumps, $\langle\tau_{\mathrm{jump}}\rangle$. Finally, we take an inverse of it to get $\kappa_0 = \langle\tau_{\mathrm{jump}}\rangle^{-1}$. We also calculate the number of adsorption sites per unit area, n, by averaging the number of particles per unit area in the first adsorption layer only for a central region of the solid-liquid interface. The obtained $\zeta_{\mathrm{CL}} = nk_{\mathrm{B}}T/\kappa_0\lambda$ and the evaluated slope $\zeta_{\mathrm{CL}}/\gamma$ are also listed in Table S4.

References

[1] Eunsang Lee, Hari Krishna Chilukoti, and Florian Müller-Plathe. Rebound suppression of a droplet impacting on a supersolvophobic surface by a small amount of polymer additives. *ACS Macro Lett.*, 10:192–196, 2021.

[2] A. Ghoufi and P. Malfreyt. Calculation of the surface tension from multibody dissipative particle dynamics and Monte Carlo methods. *Phys. Rev. E*, 82(1):016706, July 2010.

[3] O. H. Samuli Ollila, H. Jelger Risselada, Martti Louhivuori, Erik Lindahl, Ilpo Vattulainen, and Siewert J. Marrink. 3D Pressure field in lipid membranes and membrane-protein complexes. *Phys. Rev. Lett.*, 102(7):078101, February 2009.

[4] Emilie Bertrand, Terence D Blake, and Joël De Coninck. Influence of solid–liquid interactions on dynamic wetting: a molecular dynamics study. *J. Phys. Condens. Matter*, 21(46):464124, 2009.